Journal of Biomolecular NMR **27:** 341–349, 2003.
KLUWER/ESCOM

Measurement of residual dipolar couplings from $^{1}H^{\alpha}$ to $^{13}C^{\alpha}$ and ^{15}N using a simple HNCA-based experiment

Perttu Permi*
NMR Laboratory, Structural Biology and Biophysics Programme, Institute of Biotechnology, P.O. Box 65, University of Helsinki, FIN-00014, Helsinki, Finland

Received 2 April 2003; Accepted 10 June 2003

Key words: dipolar couplings, HNCA, NMR, proteins, scalar couplings, spin-state-selection

Abstract

Novel NMR pulse schemes for simultaneous measurement of $^{1}D_{C\alpha H\alpha}$ and $^{2}D_{NH\alpha}$ residual dipolar couplings in proteins is presented. We show that $^{2}D_{NH\alpha}$ coupling can be very useful for protein structure determination. The $^{2}D_{NH\alpha}$ coupling can be measured from ^{15}N dimension with good accuracy on a slowly relaxing TROSY resonance, utilizing HNCA-TROSY-based experiments, which concomitantly supply large $^{1}D_{C\alpha H\alpha}$ coupling. The dynamic range of $^{2}D_{NH\alpha}$ coupling is comparable to $^{1}D_{NC'}$ coupling, but instead, it also serves non-redundant information on the course of protein backbone, thanks to rotational degree of freedom with respect to peptide bond. The HNCA-TROSY-based experiments are optimal for measuring residual dipolar couplings at high magnetic fields owing to absence of rapid transverse relaxation of carbonyl carbon. The reliability of the proposed approach was tested on $^{15}N/^{13}C$ human ubiquitin. A very good correlation with ubiquitin solution as well as crystal structure, for both $^{1}D_{C\alpha H\alpha}$ and $^{2}D_{NH\alpha}$ couplings, was obtained.

Introduction

New structural parameters with concomitant progress in NMR methodology have not only extended the size-limit but also improved the structural quality of biological macromolecules assessed by NMR spectroscopy. Especially residual dipolar couplings have proven to be rich source of structural and dynamic information (Tolman et al., 1995; Tjandra and Bax, 1997; Bax and Tjandra, 1997; Annila et al., 1999; Prestegard et al., 2000; Bax et al., 2001). During past several years, a number of methods for accurate measurement of dipolar couplings have been introduced (Prestegard et al., 2000; de Alba and Tjandra, 2002; Bax et al., 2001). A vast majority of techniques have been devised for retrieving information on the course of protein's main-chain, yet often in perdeuterated samples (Ottiger et al., 1998a; Yang, et al., 1998, 1999; Permi and Annila, 2000; Permi et al., 2000a), but recently in side-chains as well (Ottiger et al., 1998b; Permi et al., 1999, 2000a; Carlmagno et al., 2000; Otting et al., 2000; Kaikkonen and Otting, 2001; Chou and Bax, 2001, Kontaxis and Bax, 2001; Mittermaier and Kay, 2001, Permi, 2001, 2002a). More recently, quantitative *J*-correlation experiments have been used for measuring long-range dipolar between amide protons (Wu and Bax, 2002), and also between amide protons and carbons (Meier et al., 2002) on perdeuterated proteins. Measurement of several dipolar couplings per amino acid residue can easily be motivated by smoothening the non-linear dependence of each individual dipolar coupling with respect to the polar angles, thanks to more uniform sampling of directions (Permi et al., 2000a). However, due to planarity of peptide bond, it is desirable to measure dipolar couplings also from non-planar internuclear direction such as $^{1}D_{C\alpha H\alpha}$ or $^{1}D_{C\alpha C\beta}$. A lack of couplings in non-redundant directions is often problematic especially for small or mostly helical proteins, preventing accurate estimation of the alignment tensor (Clore et al., 1998a,b).

*To whom correspondence should be addressed. E-mail: Perttu.Permi@helsinki.fi

It was shown recently by the groups of Fesik and Prestegard that the HNCA-E.COSY experiment can be used for determining residual dipolar couplings between $^1H^N(i)$ and $^1H^\alpha(i)$ (Cai et al., 1999; Tian et al., 2001). Although dipolar coupling can be rather large between amide and alpha proton, it is necessary to measure this coupling from the ^1H dimension. The unresolved dipolar couplings contribute significantly to linewidth in the proton dimension, which hampers accurate determination of the desired coupling. Systematic errors are also likely to occur in larger proteins, since the $^1H^\alpha$ spin flips during back transfer from $^{13}C^\alpha$ to $^1H^N$ results in measured couplings underestimating their true values (Wand and Bax, 1996; Cai et al., 1999). On the other hand, as internuclear distance between two protons is not fixed, the energy term in structure calculation algorithms depends also on the internuclear distance. In this paper we show that a modified HNCA-E.COSY experiment can be employed for measuring not only a large residual dipolar coupling between $^{13}C^\alpha(i)$ and $^1H^\alpha(i)$ spins but smaller coupling between the $^{15}N(i)$ and $^1H^\alpha(i)$ spins as well. The internuclear distance between amide nitrogen and alpha proton is nearly equal to that between amide proton and alpha carbon. Based solely on this fact and the gyromagnetic ratio between nitrogen and carbon, it can be estimated that dipolar contribution to this two-bond coupling is comparable to $^1D_{NC'}$, suggesting that $^2D_{NH}\alpha$ should be useful for protein structure refinement. This depends, of course, on the accuracy this intrinsically small coupling can be measured in practice. In the case of determining $^2D_{NH}\alpha$, the coupling is measured from the ^{15}N dimension on a slowly relaxing TROSY component. The linewidth in the ^{15}N dimension is considerably smaller than in the ^1H dimension, where unresolved dipolar contributions from remote protons induce additional line broadening. Thus, residual dipolar couplings can be measured significantly higher accuracy from the ^{15}N dimension in comparison with the ^1H dimension, especially on protonated samples.

Description of the pulse sequences

The pulse schemes presented in this paper are modifications of the famous HNCA-E.COSY experiment (Seip et al., 1992), originally employed for the measurement of $^3J_{H^NH}\alpha$ scalar coupling. In the following description of the pulse schemes, we elaborate solely on the differing parts of the proposed approaches. The HNCA(*J*-CAHAN)-TROSY pulse scheme devised for measuring $^1(J + D)_{C\alpha H\alpha}$ and $^2(J + D)_{NH}\alpha$ from an $^{13}C^\alpha$, ^{15}N, $^1H^N$ correlation spectrum is shown in Figure 1A. The experiment starts with the INEPT transfer from $^1H^N$ to the directly bound ^{15}N spin. The relevant density operator at time point *a* can be described by the corresponding product operator $H^N(i)_zN(i)_x$. During the ensuing t_2 evolution period, implemented in a semi-constant time TROSY manner (Logan et al., 1993; Pervushin et al., 1997; Permi and Annila, 2000), the two-bond coupling evolution between $^{15}N(i)$ and $^1H^\alpha(i)$ takes place simultaneously with the $^{15}N(i)$ chemical shift. One- and two-bond couplings from the $^{15}N(i)$ spin to neighboring $^{13}C^\alpha(i)$ and $^{13}C^\alpha(i\text{-}1)$ spins evolve during the delay $2T_a$. At time point *b*, the $90°(^{13}C^\alpha)$ pulse converts the desired $H^N(i)_zN(i)_yC^\alpha(i)_z$ coherence into the $H^N(i)_zN(i)_yC^\alpha(i)_y$ multiple quantum coherence. Omitting the corresponding $H^N(i)_zN(i)_yC^\alpha(i\text{-}1)_y$ coherence leading to sequential correlation for the sake of clarity, the relevant density operator, at time point *b*, is

$$\begin{aligned}
&\sigma_b = \\
&4HN_z(i)N_y(i)C^\alpha_y(i)\cos(\pi^2 J_{N(i)H\alpha(i)}t_2)\cos(\omega_{N(i)}t_2) \\
&+ 8HN_z(i)N_x(i)C^\alpha_y(i)H^\alpha_z(i)\sin(\pi^2 J_{N(i)H\alpha(i)}t_2) \\
&\quad \cos(\omega_{N(i)}t_2) + 4HN_z(i)N_x(i)C^\alpha_y(i) \\
&\quad \cos(\pi^2 J_{N(i)H\alpha(i)}t_2)\sin(\omega_{N(i)}t_2) \\
&+ 8HN_z(i)N_y(i)C^\alpha_y(i)H^\alpha_z(i)\sin(\pi^2 J_{N(i)H\alpha(i)}t_2) \\
&\quad \sin(\omega_{N(i)}t_2).
\end{aligned}$$

During the following t_1 period, the chemical shift of $^{13}C^\alpha$ spin is recorded concomitantly with the $^1J_{C\alpha H\alpha}$ coupling evolution. After t_1 evolution, the density operator can be given (time point *c*).

$$\begin{aligned}
&\sigma_c = \\
&4HN_z(i)N_y(i)C^\alpha_y(i)\cos(\pi^2 J_{N(i)H\alpha(i)}t_2)\cos(\omega_{N(i)}t_2) \\
&\quad \cos(\pi^1 J_{C\alpha_{(i)}H\alpha_{(i)}}t_1)\cos(\omega_{C\alpha_{(i)}}t_1) \\
&+ 8HN_z(i)N_y(i)C^\alpha_y(i)H^\alpha_z(i)\cos(\pi^2 J_{N(i)H\alpha(i)}t_2) \\
&\quad \cos(\omega_{N(i)}t_2)\sin(\pi^1 J_{C\alpha_{(i)}H\alpha_{(i)}}t_1)\sin(\omega_{C\alpha_{(i)}}t_1) \\
&+ 8HN_z(i)N_x(i)C^\alpha_y(i)H^\alpha_z(i)\sin(\pi^2 J_{N(i)H\alpha(i)}t_2) \\
&\quad \cos(\omega_{N(i)}t_2)\cos(\pi^1 J_{C\alpha_{(i)}H\alpha_{(i)}}t_1)\cos(\omega_{C\alpha_{(i)}}t_1) \\
&+ 4HN_z(i)N_x(i)C^\alpha_y(i)\sin(\pi^2 J_{N(i)H\alpha(i)}t_2) \\
&\quad \cos(\omega_{N(i)}t_2)\sin(\pi^1 J_{C\alpha_{(i)}H\alpha_{(i)}}t_1)\sin(\omega_{C\alpha_{(i)}}t_1) \\
&+ 4HN_z(i)N_x(i)C^\alpha_y(i)\cos(\pi^2 J_{N(i)H\alpha(i)}t_2) \\
&\quad \sin(\omega_{N(i)}t_2)\cos(\pi^1 J_{C\alpha_{(i)}H\alpha_{(i)}}t_1)\cos(\omega_{C\alpha_{(i)}}t_1) \\
&+ 8HN_z(i)N_x(i)C^\alpha_y(i)H^\alpha_z(i)\cos(\pi^2 J_{N(i)H\alpha(i)}t_2) \\
&\quad \sin(\omega_{N(i)}t_2)\sin(\pi^1 J_{C\alpha_{(i)}H\alpha_{(i)}}t_1)\sin(\omega_{C\alpha_{(i)}}t_1) \\
&+ 8HN_z(i)N_y(i)C^\alpha_y(i)H^\alpha_z(i)\sin(\pi^2 J_{N(i)H\alpha(i)}t_2) \\
&\quad \sin(\omega_{N(i)}t_2)\cos(\pi^1 J_{C\alpha_{(i)}H\alpha_{(i)}}t_1)\cos(\omega_{C\alpha_{(i)}}t_1) \\
&+ 4HN_z(i)N_y(i)C^\alpha_y(i)\sin(\pi^2 J_{N(i)H\alpha(i)}t_2)\sin(\omega_{N(i)}t_2) \\
&\quad \sin(\pi^1 J_{C\alpha_{(i)}H\alpha_{(i)}}t_1)\sin(\omega_{C\alpha_{(i)}}t_1).
\end{aligned}$$

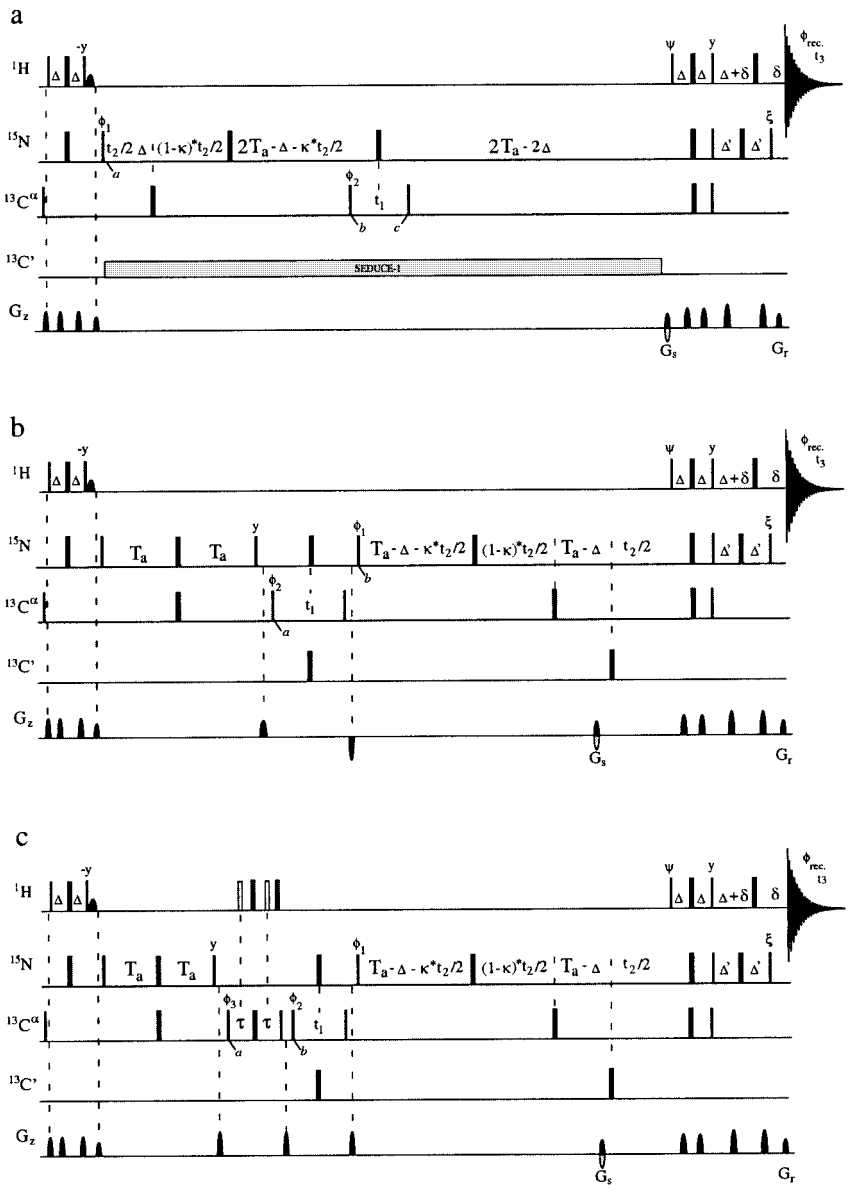

Figure 1. Pulse sequences for the simultaneous measurement of $^{1}(J+D)_{C\alpha H\alpha}$ and $^{2}(J+D)_{NH\alpha}$ scalar and residual dipolar couplings in ^{15}N, ^{13}C labeled proteins. Narrow (wide) bars correspond to 90°(180°) pulses, with phase x unless otherwise indicated. Half-ellipses denote water selective 90° pulses. All 90°(180°) pulses for $^{13}C'$ and $^{13}C^{\alpha}$ are applied with a strength of $\Omega/\sqrt{15}$ ($\Omega/\sqrt{3}$), where Ω is the frequency difference between the centers of the $^{13}C'$ and $^{13}C^{\alpha}$ regions. The semi-selective decoupling of $^{13}C'$ resonances was obtained utilizing SEDUCE-1 profile (McCoy and Mueller, 1992). The ^{1}H, ^{15}N, $^{13}C'$, and $^{13}C^{\alpha}$ carrier positions are 4.7 (water), 120 (center of ^{15}N spectral region), 55 ppm (center of $^{13}C^{\alpha}$ spectral region) and 175 ppm (center of $^{13}C'$ spectral region), respectively. Pulsed field gradients are inserted as indicated for coherence transfer pathway selection and residual water suppression. The delays employed are: $\Delta = 1/(4J_{NH})$; $\Delta' = \Delta + \delta/2$; $T_a = \sim$12–14 ms; $\tau = 1/(4J_{CH})$; $\delta = G_r+$ field recovery delay; $0 \leqslant \kappa \leqslant (2T_a - \Delta)/t_{2,max}$ (for scheme a); $0 \leqslant \kappa \leqslant (T_a - \Delta)/t_{2,max}$ (for schemes b and c). (a) the HNCA(*J*-CAHAN)-TROSY scheme. Phase cycling: $\phi_1 = 2(y), 2(-y)$; $\phi_2 = x, -x$; $\phi_3 = 4(x), 4(y)$; $\phi_{rec.} = x, 2(-x), x, -x, 2(x), -x$. Quadrature detection in the F_1-dimension is obtained by altering the phase of ϕ_2 according to States-TPPI (Marion et al., 1989). For quadrature detection in F_2, two data sets are collected (I): $\psi = x$; $\xi = y$, (II): $\psi = -x$; $\xi = -y$ with simultaneous change in gradient polarity (Weigelt, 1998; Loria et al., 1999). The data processing is according to sensitivity enhanced method (Kay et al., 1992). Gradient strengths (durations) are optimized for the highest sensitivity: $G_s = 30$ G/cm (1.25 ms), $G_r = 29.6$ G/cm (0.125 ms). (b) An alternative HNCA(*J*-CAHAN)-TROSY scheme. All parameters as in (a) except for phase cycling $\phi_1 = 2(y), 2(-y)$; $\phi_2 = x, -x$; $\phi_{rec.} = x, 2(-x), x$. Quadrature detection in the F_1-dimensions is obtained by altering the phase of ϕ_2 according to States-TPPI. (c) the HNCA(α/β-*J*-CAHAN)-TROSY experiment. The in- and antiphase data sets are recorded in an interleaved manner and subsequently added and subtracted to separate the multiplet components into two subspectra. All parameters as in (b) except for phase cycling for the in-phase spectrum: $\phi_1 = y$; $\phi_2 = x, -x$; $\phi_3 = 2(x), 2(-x)$; $\phi_{rec.} = x, 2(-x), x$; for the antiphase spectrum: $\phi_3 = 2(y), 2(-y)$. Quadrature detection in the F_1-dimensions is obtained by altering the phase of ϕ_2 according to States-TPPI.

Subsequently, the latter 90°($^{13}C^{\alpha}$) pulse flanking the t_1 period converts the desired magnetization component back to ^{15}N single quantum coherence, which is refocused during the subsequent delay $2T_a$. Ultimately, the magnetization is transferred back to amide proton utilizing gradient selected, sensitivity enhanced TROSY scheme (Weigelt, 1998; Loria et al., 1999). It is worth mentioning that no water flip-back version of the TROSY scheme is used. In this way, the emerging E. COSY pattern in the ^1H dimension collapses i.e., those operators that are antiphase with respect to the H^{α} spin in Equation [σ_c] become unobservable. This ensures that no complications for precise determination of $^2J_{NH}\alpha$ arise from an additional offset of cross peaks in proton dimension. Thus, detectable signal prior to acquisition corresponds to the magnetization modulated by terms $\exp(\omega_N t_2)\cos(\pi^2 J_{NH}\alpha t_2)\cos(\omega_C\alpha t_1)\cos(\pi^1 J_{C\alpha H\alpha} t_1)$ and $\exp(\omega_N t_2)\sin(\pi^2 J_{NH}\alpha t_2)\sin(\omega_C\alpha t_1)\sin(\pi^1 J_{C\alpha H\alpha} t_1)$ during the course of experiment.

After Fourier transform, we obtain a three-dimensional spectrum with correlations appearing at $\omega_C\alpha(i) \pm\pi^1 J_{C\alpha H\alpha}$, $\omega_N(i) \pm\pi^2 J_{NH}\alpha$, $\omega_{H^N}(i)$. Hence, large $^1J_{C\alpha H\alpha}$ can be measured from the difference in splitting in the $^{13}C^{\alpha}$ dimension, whereas $^2J_{NH}\alpha$ can be determined from the orthogonal ^{15}N dimension on the familiar E.COSY pattern as long as $^1J_{C\alpha H\alpha}$ splitting is resolved. The corresponding sequential cross peaks emerges at $\omega_C\alpha(i\text{-}1) \pm\pi^1 J_{C\alpha H\alpha}$, $\omega_N(i) \pm\pi^3 J_{NH}\alpha$, $\omega_{H^N}(i)$ allowing determination of $^3J_{NH}\alpha$ in a favorable cases.

An alternative approach for determination of $^1J_{C\alpha H\alpha}$ and $^2J_{NH}\alpha$ is presented in Figure 1b. It is conceptually similar to the pulse sequence in Figure 1a. In this latter scheme, the magnetization is first transferred to the $^{13}C^{\alpha}$ spin in an analogous manner to the HNCA-TROSY experiment (Salzmann et al., 1998). Thus, at time point *a*, the desired magnetization component is in the form of $H^N(i)_z N(i)_z C^{\alpha}(i)_y$ single quantum coherence. During the t_1 period, the $^{13}C^{\alpha}$ chemical shift modulates simultaneously with $^1J_{C\alpha H\alpha}$. Then the magnetization is converted back to ^{15}N single quantum coherence (time point *b*), which is followed by the labeling of ^{15}N chemical shift during the t_2 period, again implemented in the semi-constant manner. Also the coupling between the $^{15}N(i)$ and the passive $^1H^{\alpha}(i)$ spin is free to modulate during the t_2 period, ultimately leading to the E.COSY pattern similar to the outcome of pulse scheme in Figure 1A. Finally, the magnetization is transferred back to amide proton single quantum coherence utilizing sensitivity enhanced, gradient-selected TROSY scheme.

In order to reduce the time $^{13}C^{\alpha}$ spin being in transverse plane, the partly overlapping $^{13}C^{\alpha}-^1H^{\alpha}$ doublet components can be separated into two subspectra by the spin-state selective filtering (Yang and Nagayma, 1996; Meissner et al., 1997; Ottiger et al. 1998a; Yang et al., 1998; Permi et al., 2000b). The filter can be inserted into the HNCA(α/β-*J*-CAHAN)-TROSY pulse sequence prior to the t_1 evolution period (Figure 1c) without compromising the TROSY effect as demonstrated earlier for the α/β-HN(CO)CA-*J* TROSY experiment used for measuring $^1J_{C\alpha H\alpha}$ and $^3J_{NH}\alpha$ couplings, defining the dihedral angle ψ (Permi et al., 2000b). This will also reduce the number of arising cross peaks by factor of two, which might be the issue on larger highly alpha-helical proteins. To this end two experiments, referred here as to in-phase and antiphase spectra, will be recorded. For the in-phase spectrum, two 180°(^1H) pulses marked with unfilled bars are applied at the midpoints of delays τ in order to retain the desired coherence in-phase with respect to the $^1H^{\alpha}(i)$ spin i.e., to preserve $4H^N(i)_z N_z(i) C^{\alpha}_y(i)$ magnetization prior to the t_1 period. For the corresponding antiphase spectrum, the $4H^N(i)_z N_z(i) C^{\alpha}_y(i)$ coherence will be converted with respect to the $^1H^{\alpha}(i)$ spin into $8H^N(i)_z N_z(i) C^{\alpha}_y(i) H^{\alpha}_z(i)$ coherence. Thus, two 180°(^1H) pulses marked with filled bars are applied immediately before 180°($^{13}C^{\alpha}$) and 90°($^{13}C^{\alpha}$) pulses, respectively. In addition, the phase of the $90°_{\phi 3}$($^{13}C^{\alpha}$) pulse is shifted 90° with respect to the succeeding 90°($^{13}C^{\alpha}$) pulse. The ensuing gradient pulse purges a dispersive component of magnetization arising from *J*-mismatch (Permi et al., 2000b). It is worth mentioning that two 180°(^1H) pulses are employed purposely during the filter elements in order to provide highest sensitivity by maintaining TROSY effective throughout the most of the pulse sequence (Permi et al. 2000b). The cross-correlation between chemical shielding anisotropy (CSA) of $^{13}C^{\alpha}$ and dipole-dipole relaxation (DD) of $^{13}C^{\alpha}-^1H^{\alpha}$ is simultaneously suppressed by averaging relaxation rates of doublet components by the inversion of $^1H^{\alpha}$'s spin-state during the filter elements.

After addition and subtraction of in-phase and antiphase data sets, two subspectra exhibiting correlations at $\omega_C\alpha(i) + \pi^1 J_{C\alpha H\alpha}$, $\omega_N(i) - \pi^2 J_{NH}\alpha$, $\omega_{H^N}(i)$ and $\omega_C\alpha(i) - \pi^1 J_{C\alpha H\alpha}$, $\omega_N(i) + \pi^2 J_{NH}\alpha$, $\omega_{H^N}(i)$ will be obtained, enabling measurement of $^1J_{C\alpha H\alpha}$ and

$^2J_{NH}\alpha$ from the cross peak displacement in F_1 and F_2 dimensions between two subspectra, respectively.

Experimental

The proposed HNCA(*J*-CAHAN)-TROSY experiment was tested on human ubiquitin, having a molecular mass of 8.6 kDa (76 amino acid residues). The scalar couplings were measured on 1.9 mM, uniformly $^{15}N/^{13}C$-labeled ubiquitin, dissolved in 95/5% H_2O/D_2O in the sealed Wilmad 535PP NMR tube, pH = 5.8, 10 mM potassium phosphate buffer at 35 °C (Asla Ltd., Riga, Latvia). The corresponding couplings in aligned medium were measured on 0.9 mM $^{15}N/^{13}C$-labeled sample, prepared from dry ubiquitin dissolved in 95/5% H_2O/D_2O, composed of in-house prepared filamentous bacteriophage Pf1 (≈12 mg/ml) particles (Hansen et al., 1998) in a 250 µl Shigemi micro-cell. 250 mM NaCl was added to the sample in order to quench the electrostatic interaction between protein and the phage. The corresponding ^2H splitting in oriented sample was 7.8 Hz, which was measured using single pulse ^2H experiment. All spectra were recorded on a Varian Unity INOVA 800 MHz NMR spectrometer, equipped with a triple-resonance probehead and an actively shielded triple-axis gradient system. Spectra were processed using the standard VNMR 6.1 revision C software package (Varian associates, 2000).

The HNCA(*J*-CAHAN)-TROSY spectrum in water, recorded with pulse sequence depicted in Figure 1a, was collected with 60, 104 and 576 complex points using 2 transients per FID, corresponding to acquisition times of 15, 52 and 64 ms in t_1, t_2, and t_3, respectively. Data were zero-filled to 256 × 1024 × 1024 data matrix and apodized with shifted squared sine-bell functions in all three dimensions. The average signal-to-noise ratio for the 12-h experiment was ca. 80. Experimental parameters for the HNCA(*J*-CAHAN)-TROSY spectrum measured in a dilute liquid crystalline medium were identical to the spectrum measured in water, except for 8 transients used for signal accumulation. A reasonable signal-to-noise ratio, ca. 30 in average, was obtained in 48 h for the sample in phage.

Results and discussion

The proposed methods for measuring $^1J_{C\alpha H\alpha}$ and $^2J_{NH\alpha}$ couplings are subject to following considerations. The fundamental difference between the pulse schemes in Figures 1a and 1b,c is that the magnetization of interest is in the form of ^{15}N-$^{13}C^{\alpha}$ multiple quantum coherence during the t_1 evolution period in the pulse scheme of Figure 1a, whereas it is in the form of $^{13}C^{\alpha}$ single quantum coherence in the pulse sequences shown in Figures 1b,c. The former implementation enables us to utilize entire $2T_a - \Delta$ period for recording $^2J_{NH\alpha}$ coupling modulation during t_2, providing higher sensitivity and resolution. On the other hand, the spin-state-selective filtering can be implemented more easily into the latter scheme. This can useful especially on larger alpha-helical proteins, where increased spectral crowding due to $^1J_{C\alpha H\alpha}$ splittings can potentially become an issue. In addition, the t_1 evolution time can be held short, around 8–10 ms, since partly overlapping doublet components are separated into different subspectra (Yang et al., 1998; Permi et al., 2000b). Interestingly, it is also possible to suppress the sequential pathway completely by utilizing the intraresidual HNCA approach (Permi, 2002b) and in this way diminish the resonance overlap further.

The proposed methods are optimal for measuring couplings at high magnetic fields. First of all, TROSY implementation is ideal for the present purpose since no proton decoupling should be used during t_2 in any case. Secondly, the magnetization is not detected on (or relayed via) carbonyl carbon spin, which is relaxing very efficiently at the highest magnetic fields used today, compromising the improved sensitivity obtained by the TROSY approach (Permi and Annila, 2001, 2002; Permi, 2002). However, coherence transfer efficiency remains very high in a magnetization transfer pathway from the $^{15}N(i)$ spin to the intraresidual $^{13}C^{\alpha}(i)$ spin. Hence, it is judicious to evaluate that the novel methods are applicable also to medium-sized or larger proteins, where perdeuteration is not a prerequisite.

The capability of the methods for obtaining accurate $^1J_{C\alpha H\alpha}$ and $^2J_{NH\alpha}$ values depends on certain factors. Accurate determination of $^1J_{C\alpha H\alpha}$ relies on assumption that no large cross-correlation effects arise from cross-correlation between $^{13}C^{\alpha}-^1H^{\alpha}$ dipolar and $^1H^{\alpha}-^1H^{r}$ dipolar interactions ($^1H^r$ is a remote proton coupled to $^1H^{\alpha}$). These matters have been thoroughly discussed earlier and will not be repeated here since the proposed methods are subject to similar considerations (Yang et al., 1998; Permi et al., 2000b). Another obstacle for attaining accurate $^1J_{C\alpha H\alpha}$ couplings arises from homonuclear $^1J_{C\alpha C\beta}$ (∼35 Hz) coupling

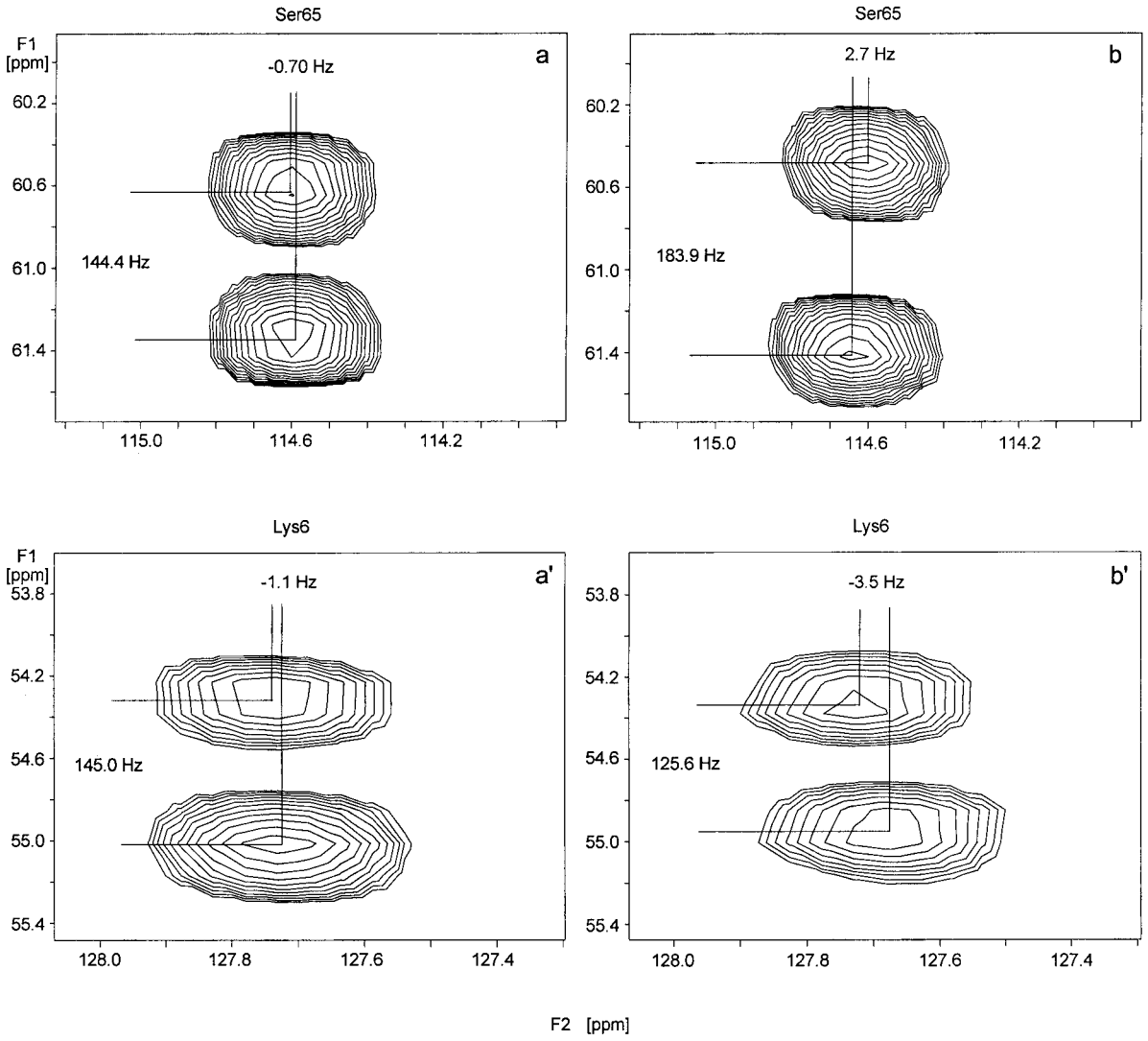

Figure 2. Representative expansion of HNCA(*J*-HACAN)-TROSY spectrum recorded from 1.9 mM uniformly ^{15}N, ^{13}C -labeled ubiquitin in water (a, a') and in phage (b, b') at 800 MHz ^{1}H frequency with the pulse scheme in Figure 1a. The spectrum a and a' show an E.COSY pattern for Ser65 and Lys6 residues with large $^{1}J_{C\alpha H\alpha}$ and a small negative $^{2}J_{NH\alpha}$ scalar couplings. The spectrum b and b' show the corresponding residues in a dilute liquid crystalline phase, composed of pf1 phage particles. Significant dipolar contributions to both $^{1}J_{C\alpha H\alpha}$ and $^{2}J_{NH\alpha}$ scalar couplings can be observed. For instance, the slope of E.COSY pattern has changed its sign for Ser65, indicating quite large positive dipolar contribution to $^{2}J_{NH\alpha}$.

evolution during t_1. For this reason, acquisition time in t_1 should not be larger than 14–16 ms. This will not create a serious problem thanks to inherently large $^{1}J_{C\alpha H\alpha}$ and high dynamic range of $^{1}D_{C\alpha H\alpha}$. An alternative solution would be the use of constant-time evolution, *albeit* with substantial loss in sensitivity. However, as demonstrated by Kay and co-workers, the cross-correlation between $^{13}C^{\alpha}$-$^{1}H^{\alpha}$ and $^{1}H^{\alpha}$-$^{1}H^{r}$ dipole-dipole interactions can cumulate in aligned phase, leading to a poorer accuracy than using the real time evolution (Yang et al., 1998). Let us now elaborate on the accuracy for determining $^{2}J_{NH\alpha}$. It can be realized that care should be taken to avoid passive spin flips between t_1 and t_2 evolution periods. Partial collapse of the E.COSY pattern due to passive spin flips results in coupling constant values, which have a bias to smaller values (Wand and Bax, 1996; Cai et al., 1999). In practice, the spin flips are serious issue only, if the passive spin is proton. However, the spin flips of $^{1}H^{\alpha}$ will not pose to a problem in the proposed

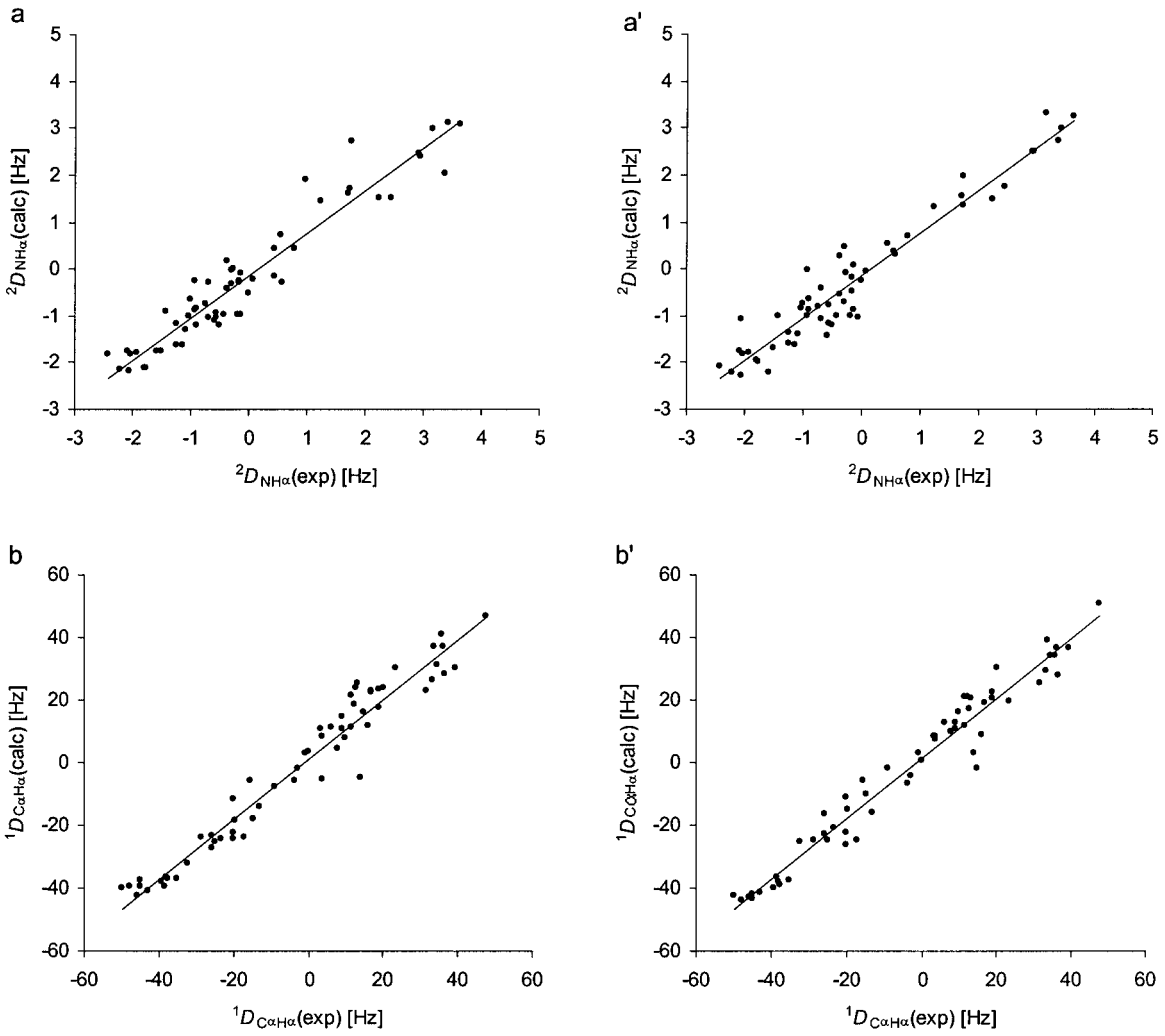

Figure 3. Correlation between the measured $^2D_{NH\alpha}$ (a) and $^1D_{C\alpha H\alpha}$ (b) residual dipolar couplings with the theoretical couplings values calculated based on ubiquitin's X-ray crystal structure 1UBQ (Vijay-Kumar et al., 1987) using program PALES (Zweckstetter and Bax, 2000). The corresponding R^2 values are 0.92 and 0.95, respectively. The corresponding correlations in (a') and (b') are calculated based on ubiquitin lowest energy NMR structure 1D3Z (Cornilescu et al., 1998). The R^2 values are 0.93 and 0.96, respectively.

methods, since the delay between t_1 and t_2 evolution periods is kept to a minimum (see Figure 1).

It is worth pointing out that if it is desired to measure $^3D_{H^NH}\alpha$ dipolar couplings simultaneously from the proton dimension using the proposed experiments, the TROSY building block should be replaced by the TROSY element devised by Yang and Kay (1999) in order to retain an E.COSY pattern in the ^{1}H dimension. Alternatively, TROSY-E.COSY element introduced by Pervushin and co-workers can be used (Vögeli and Pervushin, 2002). In general, it might also be advantageous to use conventional sensitivity-enhanced HSQC for smaller proteins with moderate TROSY effect. In that case, a selective 180° pulse for amide protons should be applied after $t_2/2$ period and spin-state-selective TROSY element should be replaced by the conventional ^{15}N-^{1}H back-INEPT in order to employ ^{15}N composite pulse decoupling during acquisition.

Figure 2 shows the representative expansions of the F_1/F_2 slices from the HNCA(*J*-CAHAN)-TROSY spectrum in water (left) and in dilute liquid crystalline phase (right), recorded using the pulse sequence in Figure 1a. The large $^1J_{C\alpha H\alpha}$ and smaller $^2J_{NH\alpha}$ couplings can be measured from the $^{13}C^\alpha$ (F_1) and ^{15}N (F_2) dimensions, respectively. The residual di-

polar couplings can be yield by subtracting the values measured in isotropic phase, from the corresponding $^1(J + D)_{C\alpha H\alpha}$ and $^2(J + D)_{NH\alpha}$ values obtained from the sample dissolved in a dilute liquid crystalline phase. As can be seen for the Lys6 and Ser65 residues, the dipolar contributions to $^2J_{NH\alpha}$ can be rather large, i.e. −2.4 and 3.6 Hz, respectively. Total of 63 $^1D_{C\alpha H\alpha}$ and $^2D_{NH\alpha}$ couplings were measured from ubiquitin, excluding 6 glycines and 3 prolines as well as the first residue in the N-terminal end. In addition, glu24 and ala46 were not observed due to exchange broadening of amide protons. The measured $^2J_{NH\alpha}$ scalar couplings in ubiquitin vary between −0.6 and −1.9 Hz and show no clear dependence on secondary structure, as expected. Residual dipolar couplings varied from −2.4 to 3.6 Hz. In order to assess viability of residual dipolar coupling data obtained using the proposed approach, experimentally measured residual dipolar couplings were compared with those predicted from ubiquitin's X-ray structure, PDB entry 1UBQ (Vijay-Kumar et al., 1987). The comparison was done by fitting the measured couplings to predicted residual dipolar couplings by using the singular value decomposition (Losonczi et al., 1999) incorporated into the program PALES (Zweckstetter and Bax, 2000). The results from this fitting are plotted in Figure 3. Very good correlation for both $^2D_{NH\alpha}$ (Figure 3a) and $^1D_{C\alpha H\alpha}$ (Figure 3b) couplings to ubiquitin's crystal structure was obtained, yielding R factors of 0.96 and 0.98, respectively. The corresponding Q values for these two dipolar couplings were quite low, 0.30 and 0.22, respectively. Fitting the measured residual dipolar couplings to ubiquitin's lowest energy NMR structure, PDB entry 1D3Z (Cornilescu et al., 1998) gave somewhat lower Q values, 0.29 (Figure 3a') and 0.21 (Figure 3b'), supporting earlier predictions that some differences between the solution and crystal structure of ubiquitin do exist.

Conclusions

In summary, we have presented a straightforward and sensitive approach for simultaneously obtaining $^1D_{C\alpha H\alpha}$ and $^2D_{NH\alpha}$ residual dipolar couplings in proteins. The novel methods are based on HNCA-type experiments, which are among the most sensitive triple-resonance experiments also at the highest magnetic fields. The magnitude of $^2D_{NH\alpha}$ is comparable to that of $^1D_{NC'}$ and it can be measured with good accuracy on the slowly relaxing TROSY cross peak from the ^{15}N dimension. We have also shown that $^2D_{NH\alpha}$ couplings can be very useful for protein structure determination as demonstrated for ubiquitin. The $^2D_{NH\alpha}$ coupling provides unique, non-redundant information on the course of protein backbone, since it does not suffer from the planarity of peptide bond. Moreover, unlike in the case of $^3D_{H^NH\alpha}$ coupling, the internuclear distance between ^{15}N(i) and $^1H^\alpha(i)$ spins for $^2D_{NH\alpha}$ coupling is fixed, whereas the rotational degree of freedom is not restricted. Our data suggests that the proposed methods will be highly useful for protein structure determination.

Acknowledgements

I am grateful to Maarit Hellman for preparing phage sample. This work was supported financially by the Academy of Finland.

References

Annila, A., Aitio, H., Thulin, E. and Drakenberg, T. (1999) *J. Biomol. NMR*, **14**, 223–230.
Bax, A. and Tjandra, N. (1997) *J. Biomol. NMR*, **10**, 289–292.
Bax, A., Kontaxis, G. and Tjandra, N. (2001) *Meth. Enzymol.*, **339**, 127–174.
Cai, M., Wang, H., Olejniczak, E.T., Meadows, R.P., Gunasekera, A.H., Xu, N. and Fesik, S. (1999) *J. Magn. Reson.*, **139**, 451–453.
Carlomagno, T., Peti, W. and Griesinger, C. (2000) *J. Biomol. NMR*, **17**, 99–109.
Chou, J.J. and Bax, A. (2001) *J. Am. Chem. Soc.*, **123**, 3844–3845.
Clore, G.M., Gronenborn, A.M. and Tjandra, N. (1998a) *J. Magn. Reson.*, **131**, 159–162.
Clore, G.M., Gronenborn, A.M. and Bax, A. (1998b) *J. Magn. Reson.*, **133**, 216–221.
Cornilescu, G., Marquardt, J.L., Ottiger, M. and Bax, A. (1998) *J. Am. Chem. Soc.*, **120**, 6836–6837.
De Alba, E. and Tjandra, N. (2002) *Prog. Nucl. Magn. Reson. Spectrosc.*, **40**, 175–197.
Hansen, M.R., Mueller, L. and Pardi, A. (1998) *Nat. Struct. Biol.*, **5**, 1065–1074.
Kaikkonen, A. and Otting, G. (2001) *J. Am. Chem. Soc.*, **123**, 1770–1771.
Kay, L.E., Keifer, P. and Saarinen, T. (1992) *J. Am. Chem. Soc.*, **114**, 10663–10665.
Kontaxis, G. and Bax, A. (2001) *J. Biomol. NMR*, **20**, 77–82.
Logan, T.M., Olejniczak, E.T., Xu, X.R. and Fesik, S.W. (1993) *J. Biomol. NMR*, **3**, 225–231.
Loria, J.P., Rance, M. and Palmer III, A.G. (1999) *J. Magn. Reson.*, **141**, 180–184.
Losonczi, J.A., Andrec, M., Fischer, M.W.F. and Prestegard, J.H. (1999) *J. Magn. Reson.*, **138**, 334–342.
Marion, D., Ikura, M., Tschudin, R. and Bax, A. (1989) *J. Magn. Reson.*, **85**, 393–399.
McCoy, M. and Mueller, L. (1992) *J. Am. Chem. Soc.*, **114**, 2108–2112.

Meier, S., Hässinger, D., Jensen, P., Rogowski, M. and Grzesiek, S. (2003) *J. Am. Chem. Soc.*, **125**, 44–45.
Meissner, A., Duus, J.Ø. and Sørensen, O.W. (1997) *J. Biomol. NMR*, **10**, 89–94.
Mittermaier, A. and Kay, L.E., (2001) *J. Am. Chem. Soc.*, **123**, 6892–6903.
Ottiger, M., Delaglio, F. and Bax, A. (1998a) *J. Magn. Reson.*, **131**, 373–378.
Ottiger, M., Delaglio, F., Marquardt, J.L., Tjandra, N. and Bax, A. (1998b) *J. Magn. Reson.*, **134**, 365–369.
Otting, G., Rückert, M., Levitt, M.H. and Moshref, A. (2000) *J. Biomol. NMR*, **16**, 343–346.
Permi, P. (2001) *J. Magn. Reson.*, **153**, 267–272.
Permi, P. (2002a) *J. Biomol. NMR*, **22**, 27–35.
Permi, P. (2002b) *J. Biomol. NMR*, **23**, 201–209.
Permi, P. and Annila, A. (2000) *J. Biomol. NMR*, **16**, 221–227.
Permi, P. and Annila, A. (2001b) *J. Biomol. NMR*, **20**, 127–133.
Permi, P. and Annila, A. (2002) *J. Magn. Reson.*, **155**, 123–130.
Permi, P., Heikkinen, S, Kilpeläinen, I. and Annila, A. (1999) *J. Magn. Reson.*, **139**, 273–280.
Permi, P., Rosevear, P.R. and Annila, A. (2000a) *J. Biomol. NMR*, **17**, 43–54.
Permi, P., Kilpeläinen, I. and Annila, A. (2000b) *J. Magn. Reson.*, **146**, 255–259.
Pervushin, K., Riek, R., Wider, G. and Wüthrich, K. (1997) *Proc. Natl. Acad. Sci. USA*, **94**, 12366–12371.
Prestegard, J.H., Al-Hashimi, H.M. and Tolman, J.R. (2000) *Quart. Rev. Biophys.*, **33**, 371–424.
Salzmann, M., Pervushin, K., Wider, G., Senn, H. and Wüthrich, K. (1998) *Proc. Natl. Acad. Sci. USA*, **15**, 181–185.
Seip, S., Balbach, J. and Kessler, H. (1992) *Angew. Chem.*, **104**, 1656–1658.
Tian, F., Valafar, H. and Prestegard, J.H. (2001) *J. Am. Chem. Soc.*, **123**, 11791–11796.
Tjandra, N. and Bax, A. (1997) *Science*, **278**, 1111–1114.
Tolman, J.R., Flanagan, J.M., Kennedy, M.A. and Prestegard, J.H. (1995) *Proc. Natl. Acad. Sci. USA*, **92**, 9279–9283.
Vijay-Kumar, S., Bugg, C.E. and Cook, W.J. (1987) *J. Mol. Biol.*, **194**, 531–544.
Vögeli, B. and Pervushin, K. (2002) *J. Biomol. NMR*, **24**, 291–300.
Wand, A.C. and Bax, A. (1996) *J. Am. Chem. Soc.*, **118**, 2483–2494.
Weigelt, J. (1998) *J. Am. Chem. Soc.*, **120**, 10778–10779.
Wu, Z. and Bax, A. (2002) *J. Am. Chem. Soc.*, **124**, 9672–9673.
Yang, D. and Nagayma, K. (1996) *J. Magn. Reson.*, **A118**, 117–121.
Yang, D. and Kay, L.E. (1999) *J. Biomol. NMR*, **14**, 273–276.
Yang, D., Tolman, J.R., Goto, N.K. and Kay, L.E. (1998) *J. Biomol. NMR*, **12**, 325–332.
Yang, D., Venters, R.A., Mueller, G.A., Choy, W.Y. and Kay, L.E. (1999) *J. Biomol. NMR*, **14**, 333–343.
Zweckstetter, M. and Bax, A. (2000) *J. Am. Chem. Soc.*, **122**, 3791–3792.